Viser Technology Pte. Ltd.
Mechanical Engineering Science
DOI: 10.33142/mes.v3i2.6727

Research Article Open Access

Process and Component Analysis on $S\text{-}CO_2$ Cooling Wall in the Coal-fired Boiler Power System

Yuanhong FAN, Danlei YANG, Guihua TANG*, Xiaolong LI

MOE Key Laboratory of Thermo-Fluid Science and Engineering, School of Energy and Power Engineering, Xi'an Jiaotong University, Xi'an 710049, China

***Corresponding Author:** *Guihua TANG, E-mail: Guihua TANG ghtang@mail.xjtu.edu.cn*

Abstract:
The supercritical carbon dioxide ($S\text{-}CO_2$) cooling wall in coal-fired boiler suffers from severe fragile crisis due to the high temperature of $S\text{-}CO_2$. The analysis of both heat transfer at process scale and cooling wall arrangement at component scale were carried out in present work. At the process scale, the difference in heat transfer performance between the smooth tube and the rifled tube were identified, especially the location of maximum outer wall temperature of cooling wall. The 1-D mathematical model for thermal-hydraulic analysis of $S\text{-}CO_2$ furnace cooling wall tubes was then developed. At the component scale, the coupled model of combustion and $S\text{-}CO_2$ heat transfer is employed for studying the thermal-hydraulic performance of rifled-spiral (R-S) and smooth-spiral (S-S) cooling wall arrangements. The maximum outer wall temperature of R-S cooling wall is 16.38℃ lower while the pressure drop increases by 2.33 times compared with the S-S cooling wall. Considering the pressure drop penalty on cycle efficiency of $S\text{-}CO_2$ boiler power system, the R-S cooling wall is not recommended, while the S-S cooling wall should be carefully arranged in $S\text{-}CO_2$ boilers.
Keywords: *thermal fragile; heat transfer; correlation; cooling wall arrangement; spiral*

Table 1 Prime table

	Nomenclatur	SCW	Supercritical water
Bo	Buoyancy parameter	T	Temperature (℃)
d	Inner diameter (mm)	U	Circumference (mm)
D	Outer diameter (mm)	x	Coordinate (mm)
f	Friction coefficient		Greek letters
g	Gravity acceleration (m • s^{-2})	α	Angle (°)
G	Mass flux (kg • m^{-2} • s^{-1})	δ	Thickness (mm)
h	Enthalpy (kJ • kg^{-1})	λ	Thermal conductivity (W • m^{-1} • K^{-1})
L	Length (mm)	ρ	Density (kg • m^{-3})
m	Mass flow (kg • s^{-1})	φ	View factor
Nu	Nusselt number		Subscripts
P	Pressure (MPa)	ave	Average
q	Heat flux (kW • m^{-2})	b	Bulk
r	Inner radius diameter (mm)	f	Friction
R	Outer radius diameter (mm)	in	Inlet
Re	Reynold number	iso	Isothermal
s	Pitch diameter (mm)	max	Maximum
$S\text{-}CO_2$	Supercritical carbon dioxide	w	Wall

1 Introduction

Due to its high efficiency [1] and compactness, the supercritical carbon dioxide ($S\text{-}CO_2$) Brayton cycle has been considered as one of the promising candidates in the coal-fired power conversion systems [2]. For the engineering design of $S\text{-}CO_2$ coal-fired power system,

Received on October 17, 2021; Accepted on December 12, 2021

one of the major issues lies in the thermal-hydraulic design of cooling wall in boilers, e.g. the prevention of thermal fragile and the circumferentially average heat transfer prediction for a single tube at the process scale, and the arrangement of the $S\text{-}CO_2$ cooling wall at the component scale.

Firstly, at the process scale, there exist restraints to the heat transfer for an actual $S\text{-}CO_2$ cooling wall tube: (1) circumferentially non-uniform heating condition, (2) large tube diameter (d), and (3) large mass flux (G). However, few work concerns the aforementioned issues [3]. The test parameters in typical experiments for the $S\text{-}CO_2$ heat transfer are presented in Table 2. We can see that the test tube diameter d is lower than 10 mm and the mass flux G is within a moderate range. Moullec et al. [4] designed the $S\text{-}CO_2$ cooling wall tube with d of 50-70 mm. In contrast, Xu et al. [5-6] suggested that although the tube with large d can theoretically alleviate the pressure drop in cooling wall, its reliability under such working conditions of high pressure and temperature cannot be ensured. Thus, a traditional range of 25-40 mm was recommended. Meanwhile, the large G in the $S\text{-}CO_2$ cooling wall was mainly caused by the low enthalpy difference of $S\text{-}CO_2$ in heaters in $S\text{-}CO_2$ power system [5]. Generally, the large G was accompanied with the large pressure drop [7], further leading to the reduction in cycle efficiency. Thus, aiming to solve this problem, some researchers employed the partial flow strategy [8-9] so that the G of $S\text{-}CO_2$ in cooling wall can be within a reasonable range of 1500-2500 kg m^{-2} s^{-1}.

Table 2 Experimental parameters in literature

Authors	*d*, mm	*P*, MPa	*G*, kg m^{-2} s^{-1}	*q*, kW m^{-2}
Tanimizu et al. [10]	8.7	7.5-9.0	185-285.97	16-64
Jiang et al. [11]	2	8.58-9.62	6.29-6.63	4.49-81
Liao et al. [12]	0.7-2.16	7.4-12	Re=(1-20) $\cdot 10^4$	10-200
Kim et al. [13]	4.5	7.46-10.26	208-874	38-234
Jiang et al. [14]	0.948-4	8.53-9.5	Re=1743-25011	2.593-108
Li et al. [15]	2	7.8-9.5	Re=3800-20000	6.50-51.96
Bae et al. [16]	6.32	7.75-8.12	285-1200	30-170
Gupta et al. [17]	8	7.4-8.8	900-3000	16-615

The smooth tube and the rifled tube are two dominant tube configurations in actual boilers [18–20]. However, the heat transfer of $S\text{-}CO_2$ in the rifled tubes are less concerned yet. Li et al. [21] studied the $S\text{-}CO_2$ inside the rifled tubes and suggested that the inner ribs can destroy the boundary layer to weaken the negative effects of buoyancy effect. Meanwhile, the heat transfer of supercritical water (SCW) inside the rifled tubes was investigated broadly, which would be helpful for understanding $S\text{-}CO_2$. Shen et al. [19] found a positive impact of inner ribs on the heat transfer of SCW. Gu et al. [22] found that the heat transfer of SCW is closely related to the ribs. Yang et al. [23] found a high flow resistance caused by the inner ribs. Whereas, note that all the above-mentioned works mainly focus on the heat transfer in the near-critical region. For the $S\text{-}CO_2$ cooling wall, the working conditions are far away from the critical point as $T_{in} > 450$ ℃ and $P_{in} \approx 30$ MPa. Moreover, as the scale of the cooling wall tube is much less than that of the combustion chamber, a simplified thermal-hydraulic tube model for predicting the maximum outer wall temperature and average outer wall temperature is essential to engineering design.

In addition to the thermal-hydraulic analysis of $S\text{-}CO_2$ at the process scale, the detailed analysis of $S\text{-}CO_2$ cooling wall arrangement is essential. Yang et al. [24] studied the 300 MW $S\text{-}CO_2$ boiler by a coupled simulation between the $S\text{-}CO_2$ heating and the combustion. Yang et al. [25], our previous work, provided both 1-D and 3-D coupled simulation of $S\text{-}CO_2$ cooling wall and proposed the "cold $S\text{-}CO_2$-hot fire matching and cascaded temperature control" method guiding the $S\text{-}CO_2$ cooling wall arrangement under partial flow strategy [5]. The method of $S\text{-}CO_2$ cooling wall arrangement in ref [25] was further proved with high reliability by Zhou et al. [7-8]. However, all the existing works for the $S\text{-}CO_2$ cooling wall are based on the smooth tube, and the rifled tube is not concerned. Moreover, the spiral cooling wall layout with the smooth or the rifled tube is widely used in the steam boiler, while the open literature concerning $S\text{-}CO_2$ cooling wall is limited to the vertical layout. Therefore, the spiral arrangement for both smooth and rifled cooling walls in $S\text{-}CO_2$ boiler needs to be examined, especially considering both thermal safety and pressure drop penalty on cycle efficiency.

The rest of the paper is organized as below. In Sec. 2, the three-dimensional numerical model for $S\text{-}CO_2$ heat transfer in both smooth tube and rifled tube and the coupled simulation method between $S\text{-}CO_2$ heating and combustion are demonstrated. The heat transfer performance is discussed in detail in Sec. 3. In Sec. 4, the arrangement of rifled-spiral R-S and smooth-spiral S-S cooling walls for $S\text{-}CO_2$ boiler is discussed. A brief conclusion is finally given in Sec. 5.

2 Numerical model and validation

2.1 3-D $S\text{-}CO_2$ heat transfer model inside smooth and rifled tubes

The numerical model of $S\text{-}CO_2$ flowing in smooth tube is quite similar to our previous work [26]. Firstly, the circular tubes made of stainless steel 316L were selected for the smooth tube and the rifled tube. The typical geometric parameters of the tubes are presented in Table 3. Particularly, the mesh of fluid region at the cross section for the rifled tube is presented in Figure 1. Four rectangular ribs with depth of 0.85 mm and width of 2.5 mm are arranged uniformly in the inner rifled tube. And the helix angle of the inner ribs is 30°. An additional isothermal section was also adopted in the present physical configuration. Secondly, the Shear Stress

Transport (SST) k-ω turbulent model was employed to solve the turbulent flow and heat transfer for S-CO_2. The model validation is shown in Figure 2 and a good agreement with available experimental data for both smooth and rifled tubes is found. Note that Figure 2a and Figure 2b stand for the high performance of SST k-ω turbulent model at near-critical region while Figure 2c further indicates a high reliability at the far-critical region. Thirdly, considering the non-uniform distribution of heat flux along the circumferential direction of the tube, the view factor of $\phi = q_{local} / q_{max}$ is adopted to model the non-uniform heat flux on the outer wall of tubes, as shown in Figure 3. Note that the view factor is calculated by a self-developed subroutine program in FLUENT based on the theoretical formulas in ref [27]. For the inner wall, the coupled thermal boundary condition and non-slip velocity boundary condition are utilized. Besides, the boundary conditions of the mass flow inlet and the pressure outlet are employed, as required by the NIST real gas model [28]. Finally, the grid independency is checked and the optimal grid numbers for smooth tube and rifled tube are 3.67 million and 4.89 million, respectively, as shown in Table 4.

Table 3 Geometric parameters of the smooth and rifled tubes

Tube	d/mm	D/mm	s/mm	L_{iso} / d_i	L_{heated} / d_i
Smooth tube	38	49.2	78	79	184
Rifled tube	38	49.2	78	79	184

Table 4 Grid independency test results

Tube	Total grid number/ $\times 10^6$	Mean relative error of Nu along the tube/ %
Smooth tube	1.37	-3.96
	2.29	-1.24
	3.08	1.67
	3.67	0.81
	4.36	0
Rifled tube	1.94	-2.64
	2.78	2.09
	3.67	1.13
	4.89	0.56
	5.91	0

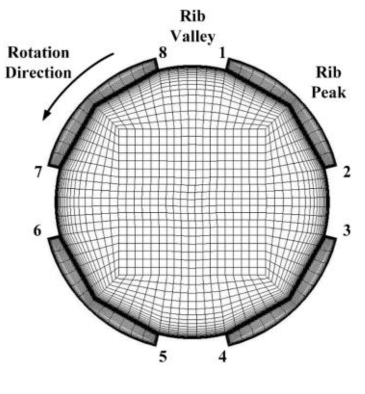

Figure 1 Cross section mesh of the rifled tube

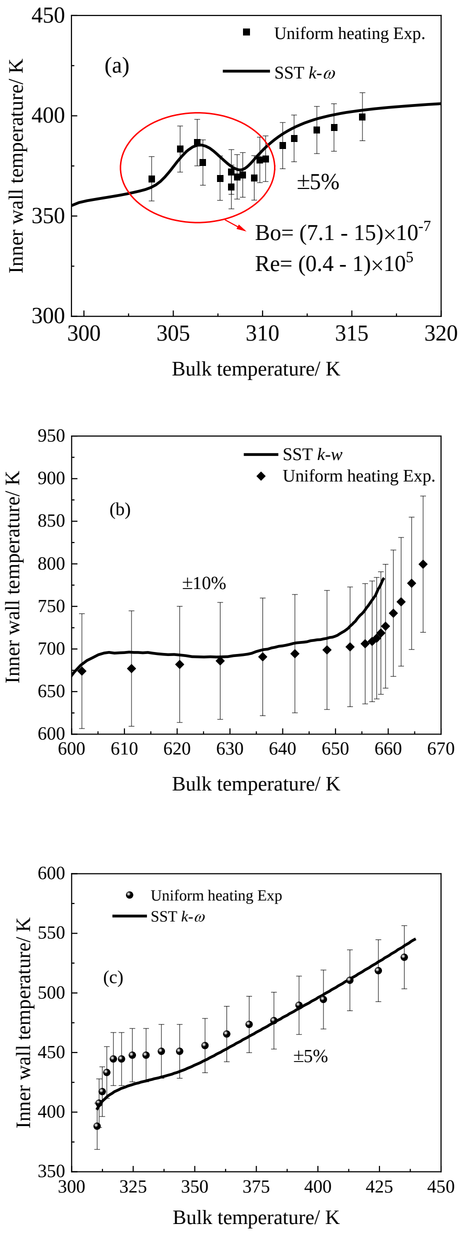

Figure 2 Comparisons between available experimental data and present predictions for (a) smooth tube [13], (b) rifled tube [23], and (c) smooth tube at far-critical region [29]

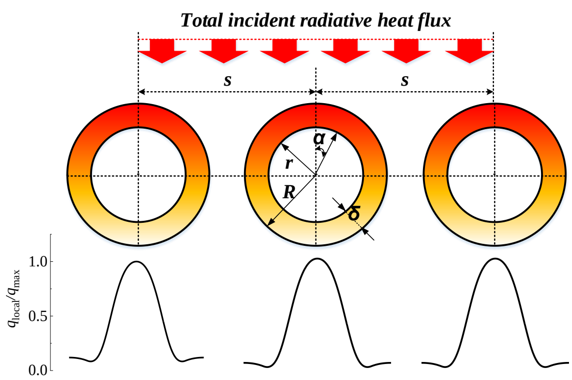

Figure 3 Non-uniform heat flux applied on the outer wall of tubes using the φ of q_{local} / q_{max}

2.2 1-D coupled simulation between S-CO_2 heating and combustion

The coupled model of combustion and S-CO_2 heat transfer for cooling wall was presented in our previous work [25], by which the thermal-hydraulic performance of cooling wall can be calculated. Firstly, the simulation of combustion of furnaces is essential for the coupled model, by which the wall furnace wall heat flux can be obtained for further S-CO_2 heat transfer calculation. Second, the 1-D S-CO_2 heat transfer model is used for cooling wall calculation. Finally, after the iteration of the two calculation processes, the maximum temperature and pressure drop of cooling wall tubes can be captured. More details about the coupled model can be found in [25]. In this work, we will use this coupled model to calculate the R-S and S-S cooling walls in S-CO_2 boiler.

3 S-CO_2 heat transfer in smooth and rifled tubes

The comparison of the heat transfer performance of S-CO_2 between the smooth tube and the rifled tube is shown in Figure 4. Note that the working conditions are based on the 1000 MW S-CO_2 coal-fired power system in ref [30]. A small difference in the inner circumferentially average heat transfer (characterized by $T_{w,inner,ave}$) is observed, indicating a negligible effect of inner ribs of rifled tubes on the circumferentially average heat transfer of S-CO_2. Meanwhile, the outer circumferentially average wall temperature ($T_{w,outer,ave}$) for the smooth tube tends to be a little higher than that of the rifled tube. This difference in $T_{w,outer,ave}$ means that the heat conduction in the solid regions cannot be ignored. Moreover, the localized maximum wall temperature in the inner wall ($T_{w,inner,max}$) of the smooth tube is almost identical to that of the rifled tube, while the localized maximum wall temperature in the outer wall ($T_{w,outer,max}$) of the smooth tube is slightly higher than that of the rifled tube.

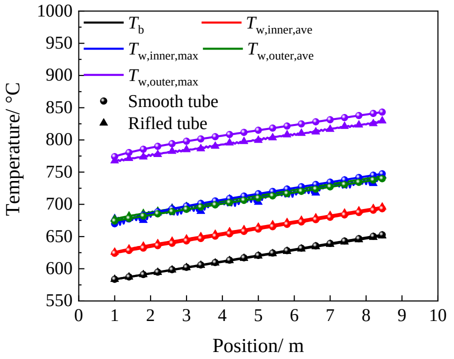

Figure 4 Comparison of heat transfer of S-CO_2 between smooth tube and rifled tube with T_{in} = 580 ℃, P_{in} = 35 MPa, q_{max} = 240 kW m^{-2} and G = 1800 kg m^{-2} s^{-1}

As shown in Figure 4, the bulk fluid temperature (T_b) and all the wall temperature almost increase linearly in the streamwise direction. Thus, the abnormal heat transfer phenomenon near the critical region does not occur at the working conditions of the S-CO_2 cooling wall. We take the distribution of the wall temperature and heat flux at 2.25 m as an example and compare the circumferential heat transfer between smooth tube and rifled tube in Figure 5. As shown in Figure 5a, both the inner wall temperature ($T_{w,inner}$) and the outer wall temperature ($T_{w,outer}$) of smooth tube show a smooth profile. In contrast, for the rifled tube, $T_{w,outer}$ shows a smooth profile, while $T_{w,inner}$ goes oscillating. This distinct distribution of $T_{w,inner}$ of rifled tube is mainly caused by the oscillating distribution of the localized heat flux on the inner wall (q_{inner}) of rifled tube, as shown in Figure 5b. Meanwhile, the smooth distribution of q_{inner} for smooth tube and the outer wall heat flux (q_{outer}) for both smooth and rifled tubes lead to the smooth distribution of the wall temperature in Figure 5a. Therefore, we can see a strong relation between the distribution of wall temperature and heat flux. Moreover, compared with the $T_{w,inner}$ of the smooth tube, the $T_{w,inner}$ of the rifled tube is more gentle since the difference between the maximum and the minimum $T_{w,inner}$ is smaller, as shown in Figure 5a. Besides, the maximum $T_{w,inner}$ in the smooth tube and the rifled tube are almost the same, while the maximum $T_{w,outer}$ of rifled tube is smaller than that of smooth tube.

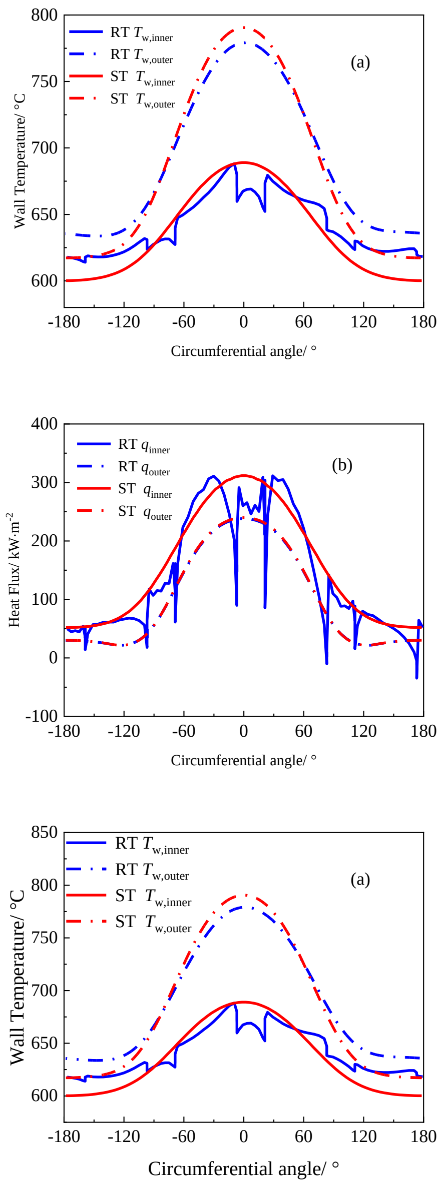

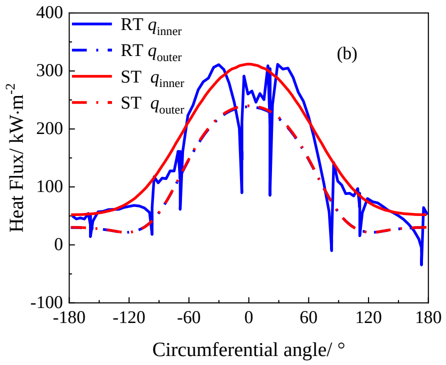

Figure 5 Circumferential distribution of (a) wall temperature and (b) heat flux on inner and outer walls for smooth tube and rifled tube in the streamwise direction of 2.25 m

$T_{w,outer,max}$ is the main concern in the analysis of thermal fragile of cooling wall. Generally, the distribution of $T_{w,outer}$ is closely related to $T_{w,inner}$. The circumferential distributions of $T_{w,inner,max}$ and $T_{w,outer,max}$ for rifled tube are further presented in Figure 6. As shown in Figure 6a, the $T_{w,inner,max}$ of rifled tube does not always occur at the heated top generatrix and shows a dispersive distribution, which is different from that of smooth tube. The $T_{w,inner,max}$ always locates near the left zone of the top generatrix. For this reason, the $T_{w,outer,max}$ of rifled tube also concentrates near the left of the top generatrix, but note that it is not that disperse as the $T_{w,inner,max}$.

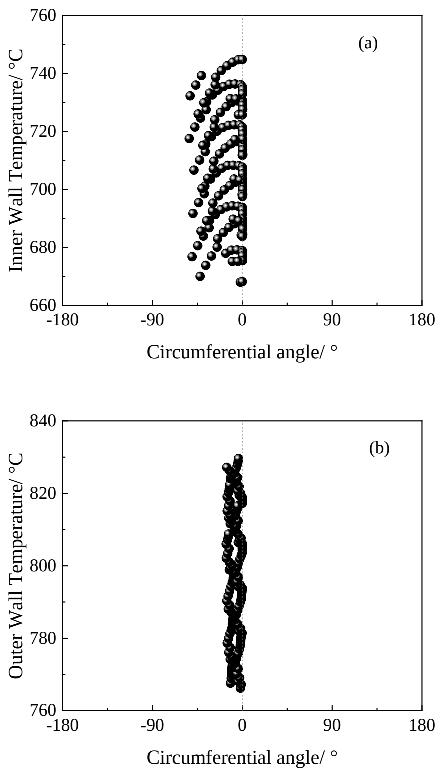

Figure 6 Circumferential distribution of (a) $T_{w,inner,max}$ and (b) $T_{w,outer,max}$ for rifled tube

To identify the relation between $T_{w,inner,max}$ and $T_{w,outer,max}$ of rifled tube, the effect of the ribs on the heat transfer of S-CO_2 in rifled tube is further discussed as shown in Figure 7. From Figure 7a, we can observe that the inner ribs lead to the rotating flow of S-CO_2, especially in the rib peak region. It indicates that the S-CO_2 in the rifled tube can be mixed more strongly than in the smooth tube. Thus, the $T_{w,inner}$ of the rifled tube can be more gentle than that of the smooth tube as shown in Figure 5a, further leading to the reduction in the maximum $T_{w,outer}$. From Figure 7b, we can observe that the points of $T_{w,inner,max}$ mostly concentrate at the intersection of rib valley and windward rib side close to the top generatrix. In contrast, the $T_{w,outer,max}$ in Figure 7c has a more even distribution. Thus, we can observe a stronger impact of heat conduction in the solid region than the inner convective heat transfer on the distribution of $T_{w,outer}$ for rifled tube.

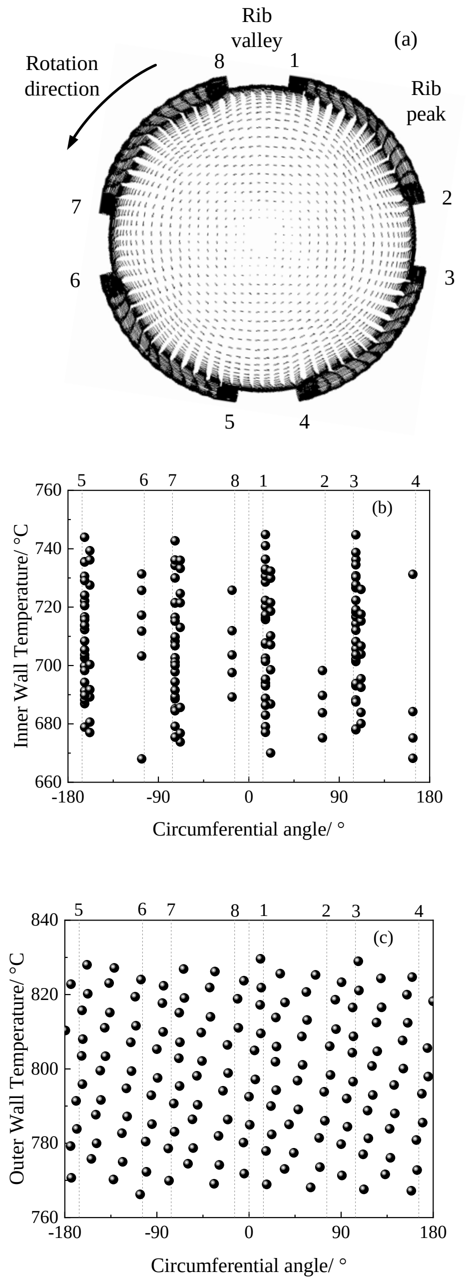

Figure 7 The impacts of inner rib distribution on the heat transfer of S-CO_2: (a) the rotating flow due to inner ribs and the distribution of (b) $T_{w,inner,max}$ and (c) $T_{w,outer,max}$

Based on the aforementioned discussion of the $S\text{-}CO_2$ flow and heat transfer, we find that both $T_{w,outer,max}$ and $T_{w,outer,ave}$ are closely related to the tube configuration (external diameter D and internal diameter d), pitch distance (S), tube solid thermal conductivity (λ_{solid}), total incident radiative heat flux value (q_{max}) and inner heat transfer coefficient (h). Thus, the empirical correlations are proposed according to the dimensional analysis method:

Smooth tube:

$$\begin{cases} T_{w,out,max} = T_b + 0.74\left(\dfrac{D}{S}\right)^{1.894}\left(\dfrac{d}{S}\right)^{-0.931}\left(\dfrac{Nu_{top} S\lambda_b}{d\lambda_{solid}}\right)^{-0.512}\left(\dfrac{q_{max} S}{\lambda_{solid}}\right) \\ T_{w,out,ave} = T_b + 0.967\left(\dfrac{D}{S}\right)^{2.470}\left(\dfrac{d}{S}\right)^{-1.648}\left(\dfrac{Nu_{ave} S\lambda_b}{d\lambda_{solid}}\right)^{-0.717}\left(\dfrac{q_{ave,out} S}{\lambda_{solid}}\right) \end{cases} \quad (1)$$

Rifled tube:

$$\begin{cases} T_{w,out,max} = T_b + 0.498\left(\dfrac{S}{d}\right)^{0.0338}\left(\dfrac{D}{d}\right)^{1.251}\left(\dfrac{Nu_{top}\lambda_b}{\lambda_{solid}}\right)^{-0.522}\left(\dfrac{q_{max} d}{\lambda_{solid}}\right) \\ T_{w,out,ave} = T_b + 2.34\left(\dfrac{S}{d}\right)^{-0.0183}\left(\dfrac{D}{d}\right)^{-1.787}\left(\dfrac{Nu_{ave}\lambda_b}{\lambda_{solid}}\right)^{-0.463}\left(\dfrac{q_{ave,out} d}{\lambda_{solid}}\right) \end{cases} \quad (2)$$

To determine the parameters along the cooling wall tube, the thermal-hydraulic correlations were incorporated into the 1-D mass, momentum and energy equations to develop the heat transfer prediction model. Firstly, the mass, momentum and energy conservation equations of the steady state $S\text{-}CO_2$ flow are solved.

Mass:

$$\frac{d\dot{m}}{dx} = 0 \quad (3)$$

Momentum:

$$\frac{dp}{dx} + \frac{dp_f}{dx} + \frac{\dot{m}^2}{A^2}\frac{d}{dx}\left(\frac{1}{\rho}\right) + \rho g = 0 \quad (4)$$

Energy:

$$\frac{dh}{dx} - \left(\frac{1}{\rho}\frac{dp}{dx} + \frac{1}{\rho}\frac{dp_f}{dx} + \frac{\int_U q dU}{\dot{m}}\right) = 0 \quad (5)$$

where p_f is the friction pressure drop. Secondly, the backward difference scheme was employed to approximate the derivatives in the conservation equations (Eqs. 3-5). The control volume of the 1-D $S\text{-}CO_2$ flow is shown in Figure 8. Finally, after obtaining the detailed parameters of $S\text{-}CO_2$ flowing inside the tube, $T_{w,outer,max}$ and $T_{w,outer,ave}$ can be calculated using Eqs. 1-2.

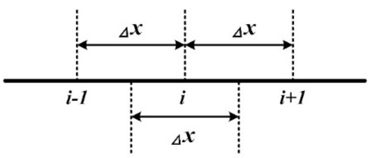

Figure 8 The 1-D $S\text{-}CO_2$ flow control volume

To validate the present model, we compared the $S\text{-}CO_2$ heat transfer results between the FLUENT 3-D simulation and the present 1-D model in Figure 9 and a good agreement is found. Therefore, the present 1-D model can be regarded as an efficient and accurate tool for the design of $S\text{-}CO_2$ furnace cooling wall.

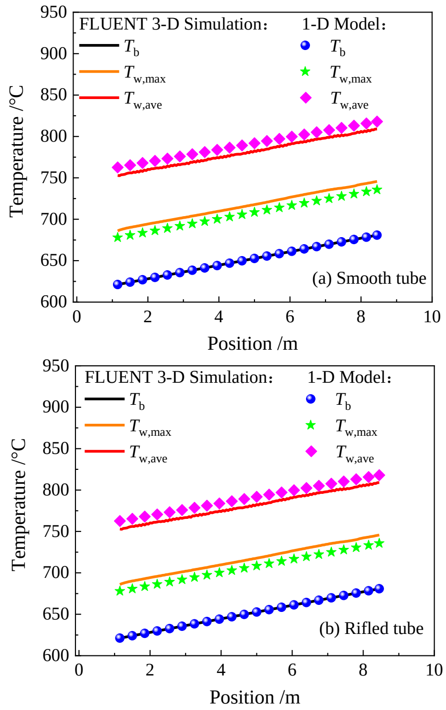

Figure 9 Comparison of temperature between FLUENT 3-D simulation and present 1-D model. (a) Smooth tube. (b) Rifled tube

4 R-S and S-S cooling wall arrangements for $S\text{-}CO_2$ boiler

The spiral cooling wall arrangement calculation is based on the coupled model of combustion and $S\text{-}CO_2$ heat transfer. In the coupled model, the cooling wall tube model can be set as smooth tube or rifled tube by changing the empirical correlations as shown in Eqs.1 and 2. To examine the R-S and smooth-spiral (S-S) cooling wall in 1000 MW $S\text{-}CO_2$ boiler, a traditional cooling wall arrangement in steam boiler is chosen, in which the integral spiral tubes cover the whole surface of the furnace wall without interruption. The inclination of spiral tube is 30°. The thermal parameters of the cooling wall are presented in Table 5.

Table 5 Thermal parameters of the cooling wall

Cooling wall	Inlet temperature/℃	Inlet pressure /MPa	Mass flow/kg·s^{-1}
S-S and R-S	552.87	35.35	6320.09

The fluid temperature and maximum outer wall temperature distributions of R-S and S-S cooling walls are presented in Figure 10. First, we can see that the maximum outer wall temperature of R-S cooling wall is lower than that in S-S cooling wall. The maximum temperature difference is up to 16.38 ℃ in the tube outlet. The rifled tube can successfully reduce the maximum outer wall temperature. Second, the $S\text{-}CO_2$

fluid temperatures are quite similar inside both cooling walls due to the same heat load. Third, the profiles of maximum outer wall temperature show an obvious drop near 20 m in the furnace height direction, where the spiral cooling walls are going through the corner of the furnace and the wall heat fluxes are quite low due to the dual circle tangential firing in the furnace. In summary, the rifled tube can improve the thermal safety of the furnace.

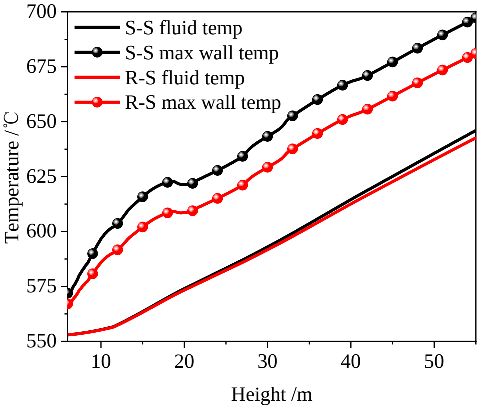

Figure 10 Fluid and maximum outer wall temperature distributions of R-S and S-S cooling wall in S-CO_2 boiler

In addition, the pressure drop penalty on cycle efficiency is essential for S-CO_2 boiler. Figure 11 shows the pressure drops of R-S and S-S cooling walls. Due to the large flow friction in the rifled tube, the pressure drop in R-S cooling wall increases by 2.33 times of that in S-S cooling wall, which will cause incredible penalty on cycle efficiency. Since the reduction in the cooling wall temperature by the rifled tube is not obvious either, it is not recommended in S-CO_2 boilers. Moreover, the pressure drop in S-S cooling wall is up to 4.10 MPa, which is extremely high. It is because we do not use the partial flow strategy and module design of the cooling wall [5]. According to the 1/8 principle [5] and 4 times of the cooling wall length, the present pressure drop of S-S cooling wall increases by 31 times of the result in our previous work [26] using partial flow strategy. Therefore, we can come to a conclusion that the S-S cooling wall should be carefully arranged in S-CO_2 boiler, while the R-S cooling wall is not recommended.

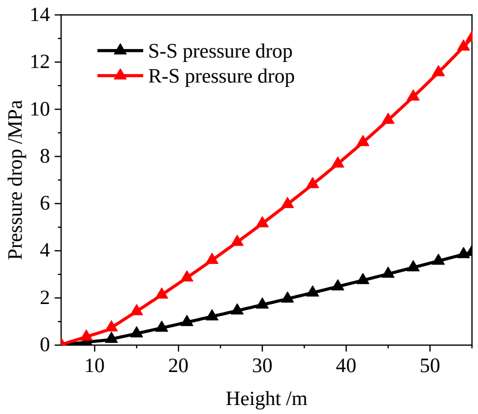

Figure 11 Pressure drops of R-S and S-S cooling walls in S-CO_2 boiler

5 Conclusions

The process and component analysis for the supercritical carbon dioxide (S-CO_2) cooling wall in coal-fired boiler was investigated, including the heat transfer performance and the S-CO_2 cooling wall arrangement. The main conclusions are as follows.

(1) The rifled tube is able to reduce the maximum outer wall temperature since it has a stronger mixing effect on S-CO_2 than the smooth tube under the non-uniform heating.

(2) The 1-D heat transfer prediction model coupled with the empirical correlations for S-CO_2 inside smooth tube and rifled tube is developed based on the 1-D steady state governing equations. A good agreement for S-CO_2 fluid flow and heat transfer prediction is found between the 1-D heat transfer prediction model and the 3-D FLUENT simulation.

(3) The coupled model of combustion and S-CO_2 heat transfer is employed for cooling wall arrangement. The maximum outer wall temperature of rifled-spiral cooling wall is 16.38 ℃ lower, while the pressure drop increases by 2.33 times compared with the smooth-spiral cooling wall. Considering both pressure drop penalty on the cycle efficiency of S-CO_2 boiler and the wall temperature reduction, the rifled-spiral cooling wall is not recommended in S-CO_2 coal-fired boilers. In addition, the smooth-spiral cooling wall should also be carefully arranged due to its extremely high pressure drop.

Author Contributions: G.H. Tang: Conceptualization, Investigation, Methodology, Funding acquisition, Project administration, Supervision, Writing – review & editing; Y.H. Fan: Formal analysis, Investigation, Methodology, Validation, Writing-original draft, Writing – review & editing; D.L. Yang: Formal analysis, Investigation, Methodology, Validation, Writing-original draft, Writing – review & editing; X.L. Li: Formal analysis.

Conflict of Interest: The authors declare that there is no conflict of interest regarding the publication of this paper.

Acknowledgments: This work was supported by the National Key Research and Development Program of China under grant number of 2017YFB0601803 and the National Natural Science Foundation of China under grant number of 51721004.

References

[1] Wang K, Li MJ, Zhang ZD, Min CH, Li P. Evaluation of alternative eutectic salt as heat transfer fluid for solar power tower coupling a supercritical CO_2 Brayton cycle from the viewpoint of system-level analysis. J Clean Prod 2021;279:123472. https://doi.org/10.1016/j.jclepro.2020.123472.

[2] Mecheri M, Le Moullec Y. Supercritical CO_2 Brayton cycles for coal-fired power plants. Energy 2016;103:758–71. https://doi.org/10.1016/j.energy.2016.02.111.

[3] Fan YH, Tang GH. Numerical investigation on heat transfer of supercritical carbon dioxide in a vertical tube under circumferentially non-uniform heating. Appl Therm Eng

2018;138:354–64. https://doi.org/10.1016/j.applthermaleng.2018.04.060.

[4] Le Moullec Y. Conceptual study of a high efficiency coal-fired power plant with CO_2 capture using a supercritical CO_2 Brayton cycle. Energy 2013;49:32–46. https://doi.org/10.1016/j.energy.2012.10.022.

[5] Xu J, Sun E, Li M, Liu H, Zhu B. Key issues and solution strategies for supercritical carbon dioxide coal fired power plant. Energy 2018;157:227–46. https://doi.org/10.1016/j.energy.2018.05.162.

[6] Liu C, Xu J, Li M, Wang Z, Xu Z, Xie J. Scale law of sCO_2 coal fired power plants regarding system performance dependent on power capacities. Energy Convers Manag 2020;226:113505. https://doi.org/10.1016/j.enconman.2020.113505.

[7] Zhou J, Zhu M, Xu K, Su S, Tang Y, Hu S, et al. Key issues and innovative double-tangential circular boiler configurations for the 1000 MW coal-fired supercritical carbon dioxide power plant. Energy 2020;199:117474. https://doi.org/10.1016/j.energy.2020.117474.

[8] Zhou J, Xiang J, Su S, Hu S, Wang Y, Xu K, et al. Key issues and practical design for cooling wall of supercritical carbon dioxide coal-fired boiler. Energy 2019;186:115834. https://doi.org/10.1016/j.energy.2019.07.164.

[9] Guo JQ, Li MJ, Xu JL, Yan JJ, Ma T. Energy, exergy and economic (3E) evaluation and conceptual design of the 1000 MW coal-fired power plants integrated with S-CO_2 Brayton cycles. Energy Convers Manag 2020;211:112713. https://doi.org/10.1016/j.enconman.2020.112713.

[10] Tanimizu K, Sadr R. Experimental investigation of buoyancy effects on convection heat transfer of supercritical CO_2 flow in a horizontal tube. Heat Mass Transf Und Stoffuebertragung 2016;52:713–26. https://doi.org/10.1007/s00231-015-1580-9.

[11] Jiang PX, Zhang Y, Xu YJ, Shi RF. Experimental and numerical investigation of convection heat transfer of CO_2 at supercritical pressures in a vertical tube at low Reynolds numbers. Int J Therm Sci 2008;47:998–1011. https://doi.org/10.1016/j.ijthermalsci.2007.08.003.

[12] Liao SM, Zhao TS. An experimental investigation of convection heat transfer to supercritical carbon dioxide in miniature tubes. Int J Heat Mass Transf 2002;45:5025–34.

[13] Kim DE, Kim MH. Experimental investigation of heat transfer in vertical upward and downward supercritical CO2 flow in a circular tube. Int J Heat Fluid Flow 2011;32:176–91. https://doi.org/10.1016/j.ijheatfluidflow.2010.09.001.

[14] Jiang PX, Xu YJ, Lv J, Shi RF, He S, Jackson JD. Experimental investigation of convection heat transfer of CO_2 at super-critical pressures in vertical mini-tubes and in porous media. Appl. Therm. Eng., vol. 24, 2004, p. 1255–70. https://doi.org/10.1016/j.applthermaleng.2003.12.024.

[15] Li ZH, Jiang PX, Zhao CR, Zhang Y. Experimental investigation of convection heat transfer of CO_2 at supercritical pressures in a vertical circular tube. Exp Therm Fluid Sci 2010;34:1162–71. https://doi.org/10.1016/j.expthermflusci.2010.04.005.

[16] Bae YY, Kim HY, Kang DJ. Forced and mixed convection heat transfer to supercritical CO_2 vertically flowing in a uniformly-heated circular tube. Exp Therm Fluid Sci 2010;34:1295–308. https://doi.org/10.1016/j.expthermflusci.2010.06.001.

[17] Gupta S, Saltanov E, Mokry SJ, Pioro I, Trevani L, McGillivray D. Developing empirical heat-transfer correlations for supercritical CO 2 flowing in vertical bare tubes. Nucl Eng Des 2013;261:116–31. https://doi.org/10.1016/j.nucengdes.2013.02.048.

[18] Li Z, Lu J, Tang G, Liu Q, Wu Y. Effects of rib geometries and property variations on heat transfer to supercritical water in internally ribbed tubes. Appl Therm Eng 2015;78:303–14. https://doi.org/10.1016/j.applthermaleng.2014.12.067.

[19] Shen Z, Yang D, Mao K, Long J, Wang S. Heat transfer characteristics of water flowing in a vertical upward rifled tube with low mass flux. Exp Therm Fluid Sci 2016;70:341–53. https://doi.org/10.1016/j.expthermflusci.2015.09.021.

[20] Li Z, Wu Y, Tang G, Zhang D, Lu J. Comparison between heat transfer to supercritical water in a smooth tube and in an internally ribbed tube. Int J Heat Mass Transf 2015;84:529–41. https://doi.org/10.1016/j.ijheatmasstransfer.2015.01.047.

[21] Li Z, Tang G, Wu Y, Zhai Y, Xu J, Wang H, et al. Improved gas heaters for supercritical CO_2 Rankine cycles: Considerations on forced and mixed convection heat transfer enhancement. Appl Energy 2016;178:126–41. https://doi.org/10.1016/j.apenergy.2016.06.018.

[22] Gu J, Zhang Y, Wu Y, Li Z, Tang G, Wang Q, et al. Numerical study of flow and heat transfer of supercritical water in rifled tubes heated by one side. Appl Therm Eng 2018;142:610–21. https://doi.org/10.1016/j.applthermaleng.2018.07.017.

[23] Yang D, Pan J, Zhou CQ, Zhu X, Bi Q, Chen T. Experimental investigation on heat transfer and frictional characteristics of vertical upward rifled tube in supercritical CFB boiler. Exp Therm Fluid Sci 2011;35:291–300. https://doi.org/10.1016/j.expthermflusci.2010.09.011.

[24] Yang Y, Bai W, Wang Y, Zhang Y, Li H, Yao M, et al. Coupled simulation of the combustion and fluid heating of a 300 MW supercritical CO_2 boiler. Appl Therm Eng 2017;113:259–67. https://doi.org/10.1016/j.applthermaleng.2016.11.043.

[25] Yang DL, Tang GH, Fan YH, Li XL, Wang SQ. Arrangement and three-dimensional analysis of cooling wall in 1000 MW S–CO_2 coal-fired boiler. Energy 2020;197:117168. https://doi.org/10.1016/j.energy.2020.117168.

[26] Fan YH, Yang DL, Tang GH, Sheng Q, Li XL. Design of S–CO_2 coal-fired power system based on the multiscale analysis platform. Energy 2021;240:122482. https://doi.org/10.1016/J.ENERGY.2021.122482.

[27] Duda P, Taler J. A new method for identification of thermal boundary conditions in water-wall tubes of boiler furnaces. Int J Heat Mass Transf 2009;52:1517–24. https://doi.org/10.1016/j.ijheatmasstransfer.2008.08.013.

[28] E.W. Lemmon, M.L. Huber, M.O. McLinden. Reference fluid thermodynamic and transport properties (REFPROP) 2007.

[29] Kline N, Feuerstein F, Tavoularis S. Onset of heat transfer deterioration in vertical pipe flows of CO_2 at supercritical pressures. Int J Heat Mass Transf 2018;118:1056–68. https://doi.org/10.1016/j.ijheatmasstransfer.2017.11.039.

[30] Sun E, Xu J, Li M, et al. Connected-top-bottom-cycle to cascade utilize flue gas heat for supercritical carbon dioxide coal fired power plant. Energy Convers Manag 2018;172:138–54. https://doi.org/10.1016/j.enconman.2018.07.017.